

An earthquake engineering approach to vibrocompaction

Approche parasismique des effets du vibrocompactage

Alain E. Holeyman – *Université Catholique de Louvain, Louvain-la-Neuve, Belgium (Formerly: Earthspectives, Irvine, USA)*

ABSTRACT: Based on the common phenomena governing liquefaction induced by an earthquake and densification induced by deep vibratory probing, an approach is suggested to evaluate the improvement potential created by vibrocompaction, borrowing concepts from earthquake engineering. An equivalent cyclic stress ratio is introduced, taking into account the direction of the shear waves, number of cycles, and repetition of probing events as governed by the probing pattern. A recent case history where a vibratory "Y-probe" was used to densify liquefiable materials in British Columbia, Canada, is reviewed. Results provided by the in situ testing performed before and after treatment confirm the general nature of conclusions that can be derived from the suggested approach.

RESUME: Sur base des phénomènes communs régissant la liquéfaction des sols induite par un tremblement de terre et la densification induite par la pénétration de profils vibrants, une approche est présentée pour évaluer l'amélioration des sols en profondeur au moyen du vibrocompactage, en empruntant des concepts utilisés en génie parasismique. Un rapport de contrainte cyclique équivalent est présenté, compte tenu de la direction des ondes de cisaillement, du nombre de cycles et de la répétition des événements de pénétration du profil vibrant résultant de la maille de compactage. Un chantier où un profil vibrant en forme d'étoile a été utilisé pour densifier des sols liquéfiables en Colombie Britannique, Canada, est passé en revue. Les résultats fournis par des essais in situ exécutés avant et après traitement du sol confirment l'allure générale des conclusions déduites de l'approche suggérée.

1 INTRODUCTION

Amongst the methods available to improve earthquake sensitive soil layers, vibrocompaction is often an attractive option because of its apparent simplicity, lack of requirement for water and backfill, and cost. Vibrocompaction at depth can be accomplished by using several vibrating tools that have been developed and patented by contractors and engineers. The system addressed in this paper is referred to as the "Y-probe," but is also known as the "TriStar probe," and is operated on the American continent by Franki.

As described by Neely and Leroy (1991), the probe consists of three long steel plates assembled 120° apart at the vertical probe axis. The plates are generally 0.5m wide and 12 to 20 m long. They are provided with horizontal ribs to enhance the transfer of energy to the surrounding soil. The probe is attached at its head to a powerful pile vibrator suspended from a crane, as shown in Fig. 1. The treatment consists in probing the particular area of a site to be densified following a regular areal pattern, generally characterized by the spacing between probing locations.

On occasion, several patterns are overlain, leading to the delivery of the densification effort in distinct passes. At each

predetermined probing location, the probe is inserted to the desired depth using maximum power, and withdrawn slowly in stages using reduced power. The insertion and withdrawal procedures have been developed over the years based on in situ assessment of improvement performance. The procedures have also been refined with the basic understanding of the coupled and de-coupled regimes that characterize the vibratory interaction between the probe and the soil.

Although it is appreciated that transfer of mechanical energy to the soil should result in its densification, it must be understood (Mitchell 1981) that liquefaction, or de-stabilization of the arrangement of particles, is a pre-requisite to densification. As a result of this fundamental understanding, soils classified as non-liquefiable on the basis of their grain size characteristics are generally not considered suitable for improvement using vibrocompaction.

Based on the common phenomena governing liquefaction during an earthquake and during Y-probe induced vibrations, an engineering approach is herein suggested to evaluate the improvement potential created by the Y-probe, borrowing from the body of knowledge now available in the field of earthquake engineering. In fact, a consistent parallel can be drawn between the effects resulting from the engineered vibrations using the Y-probe process and those caused by an earthquake. Within this proposed framework, vibrocompaction can be viewed as a seismic preloading process which must be engineered with due consideration to the design earthquake.

2 EARTHQUAKE ENGINEERING APPROACH

2.1 General Comparison

The Y-probe can be considered as a seismic source of reduced size when compared to a fault. The level of vibration induced at a particular distance from the Y-probe can be evaluated on the basis of theoretical or experimental attenuation laws, similar to those established for earthquake engineering (Campbell, 1981). The effects on the soil at a particular distance and depth can be evaluated using the concept of cyclic stress ratio, adapted to

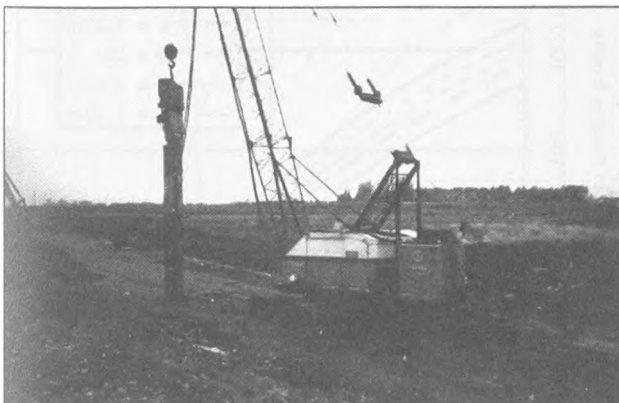


Figure 1. Deep Vibratory Probing Equipment

account for the direction of the shear waves, number of cycles, and repetition of probing events as governed by the probing pattern.

Table 1 provides a list of parameters that are known to influence soil behavior under cyclic loading and compares their typical values in the case of the design earthquake and the engineered Y-probe. This comparison shows that, within their respective zones of interest, vibration levels are of the same order of magnitude and therefore are bound to produce similar effects on soils; these effects are considered adverse during an earthquake and favorable during vibrocompaction.

Table 1. Typical Values of Attributes and Parameters characterizing Cyclic Loading

Attribute /Parameter (1)	Design Earthquake (2)	Engineered Y-probe (3)	Representative Scaling Factor (4) = (3)/(2)
Source Area	5 - 50 km ²	50 m ²	2.10 ⁻⁶
Focal Depth	2 - 10 km	10 m	2.10 ⁻³
Radius of Influence	5 - 10 km	1 - 2 m	0.2 10 ⁻³
Vibration Duration	10 - 100 s	300 - 1,500 s	20
Recurrence	0.05 - 0.50 in 100 years, at nature's whim	100 - 1,000, per design	Not Applicable
Acceleration at source	1 - 5 g	5 - 10 g	2
Acceleration at radius of influence	0.2 - 0.5 g	0.2 - 0.5 g	1
Number of cycles	5 - 20	10 ⁴ - 3.10 ⁴	2.10 ³

2.2 Attenuation Law

The attenuation relationship describes the rate at which the vibration level decreases as a function of the epicentral distance (r). Attenuation relationships used in earthquake engineering are based on instrument records and the theory of wave propagation. Although proposed mathematical laws differ due to the type of fault and scatter in the records utilized to derive them, they provide a simple means to evaluate acceleration levels as a function of the distance for several levels of earthquake magnitude (Mualchin and Jones 1992).

For the Y-probe which oscillates along its vertical axis, the attenuation is mainly governed by the geometric damping of the cylindrical waves radiating away from the probe. For an infinitely long probe operating in an elastic medium geometric damping prevails in accordance with $r^{-1/2}$. To account for the finite length of the probe and the internal soil damping, it is proposed to accentuate the attenuation by using a formula of the following type:

$$A_r = (d \cdot (1 + b \cdot d))^{-1/2} \cdot e^{-a \cdot d} \quad (1)$$

where :

A_r = Amplitude of vibration at radial distance r
 $d = (r^2 + h^2)^{1/2}$, with h = probe ribs equivalent focal depth
 b = geometric damping accentuation factor
 a = intrinsic soil damping

Results of measurements collected at various distances from the Y-probe actuated by specific vibrators operating at several frequencies are presented in the attenuation diagram of Fig. 2. A wide scatter, not unlike that generally observed from seismic

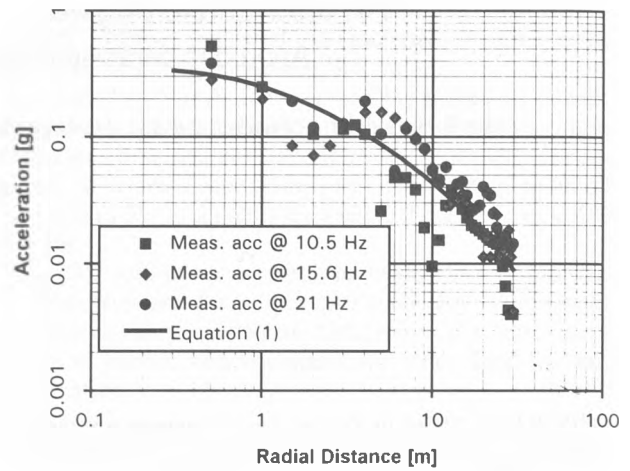


Figure 2. Attenuation Relationship

measurements, can be noted. Fig. 2 also shows the attenuation law derived using equation (1) for the following set of matching parameters : $h = 0.7\text{m}$, $b = 1/30 \text{ m}^{-1}$, and $a = 0.03 \text{ m}^{-1}$.

2.3 Recurrence

While the recurrence of an earthquake of a particular magnitude can be evaluated from a statistical or probabilistic standpoint, the number of probing events is determined from the known probing pattern. To study the cumulative effect of probing events on the equivalent acceleration felt by the soil at a particular location within a probing pattern, the attenuation law shown in Fig. 2 was convoluted with the probe radial density function corresponding to a triangular pattern of probing points. The recurrence functions derived at center points of triangular probing patterns, i.e., at the most conservative location within the pattern, are shown in Fig. 3 for probe spacings varying between 1.25 and 2.5 m.

The number of probing events represented in Fig. 3 is equivalent to the number of probes located within the radial distance corresponding to a given acceleration level. Such a diagram allows probe spacing to be converted into acceleration levels of a given recurrence (e.g., acceleration varying with probe spacing from 0.21 to 0.28 g for 3 events). It also allows one to assess the equivalent number of probes that will cause a given acceleration level to be exceeded (e.g., 3.1 to 8 events with probe spacing varying from 2.5 to 1.25 m for a given acceleration of 0.2 g). It should be noted that the recurrence of the probing events

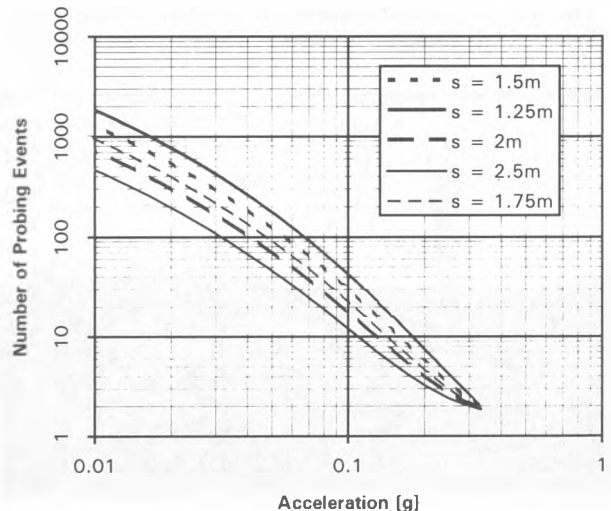


Figure 3. Acceleration recurrence

should be multiplied by the number of loading cycles characterizing each probing event to obtain the total number of cycles of a particular magnitude.

2.4 Cyclic Stress Ratio

The notion of cyclic stress ratio (cyclic shear stress divided by normal effective stress) has been introduced in earthquake engineering to assess an equivalent seismic loading with regard to liquefaction potential. The cyclic stress ratio can be calculated as a function of depth for a seismic shaking of known or assumed magnitude and ground acceleration level. This calculation is performed using wave propagation models (Schnabel et al. 1972, Finn et al. 1978), or empirical formulae (Seed and Idriss 1971). Results of such a calculation are provided in Fig. 4 for a design site shaking corresponding to magnitude $M=7$ and an acceleration $a = 0.3g$.

The cyclic stress ratio at various depths is then compared to that experimentally known to produce liquefaction under a given number of cycles, taking into account the nature, history, and, most importantly, the grain size characteristics of the soil layer considered. Also, stress ratios can be converted into threshold SPT blow counts (Seed et al. 1984) or CPT cone resistances beyond which it has been empirically established that liquefaction is unlikely. These threshold values are often used to formulate specifications for densification treatments.

The cyclic stress ratio generated by the Y-probe densification process can be readily assessed based on the equivalent cyclic shear stress corresponding to the cylindrical waves propagating away from the probe and on the effective horizontal stress. The horizontal normal stress has to be considered because the direction of the alternating cyclic shear is vertical; it is further assumed that the cyclic shear stress is uniform with depth. The vertical cyclic shear stress can be obtained by converting the accelerations of the attenuation law represented in Fig. 2 into velocities and multiplying the resulting velocities by the specific (or acoustic) impedance of the soil under vertical shear.

In the case of vibrocompaction, the equivalent cyclic stress needs to be upgraded to account for the number of cycles during a probing event (typically 20,000), which is much larger than the number of repeatable strong cycles during an earthquake (typically 15 for a magnitude 7.5 event). Based on these typical numbers of cycles, a shear stress multiplier of 1.5 was adopted to generate the equivalent stress ratio profiles represented in Fig. 4. The stress profiles shown correspond to vertical lines located at

radial distances varying from 0.7 to 6m from the probe axis. Fig. 4 shows that the cyclic stress ratio generated by the Y-probe locally exceeds that of the design earthquake.

It is of interest to note that according to the approach suggested herein, the radius of influence of treatment exceeding a given level of seismic stress, decreases with depth. Conversely, the depth at which liquefaction is induced by the Y-probe depends on the radial distance to the probe. This would imply that the concept of zone of influence should be replaced by that of volume of influence, with the understanding that the volume of influence is more conical than cylindrical.

3 CASE HISTORY

3.1 Project Description

Loose sandy layers were identified as liquefiable on a site planned for industrial development which gently sloped towards the Fraser River, in East Richmond, British Columbia, Canada. The geotechnical engineer recommended that the buildings be supported on either deep foundations or spread footings in conjunction with preloading or, as an alternative, overall site seismic stability could be improved by densification of a zone parallel to the river. The intent of this approach is to lower the risk of seismically induced liquefaction within a limited zone or berm parallel to the river to an acceptable level, thereby reducing the risk of large lateral ground movements within the site during a major seismic event.

This latter option was exercised by the owner who selected Franki to carry out the berm densification using the Y-probe method of vibrocompaction. Two berms were called for in the specifications: a west berm, covering Stations (Sta) 0+00 to 4+00, and an east berm, covering Sta 6+00 to 9+57. Each berm was 12 m wide and required densification to an average elevation of -12.50, i.e., to depths ranging from approximately 13 to 15 m, depending on the existing grade.

Based on test borings and Dynamic Penetration Tests (DPT), the subsurface conditions were reported to comprise fill over silt at the west berm and silt only at the east berm. These soils are underlain by variable sandy silt and/or silt and sand over relatively clean sand. At the west berm the soft to firm silt was generally encountered from a depth ranging between 0.5 to 2.3 m to a depth of up to 4 m and underlain by variable and/or laminated sandy silt, silt and sand or silty sand to depths ranging between 4.0 and 7.8 m. In general, the above sequence was underlain by the loose to medium dense sand of seismic concern to depths of 18.6 m, below which it became dense to very dense. Ground water was observed during drilling at depths ranging between 0.7 to 2.5 m, or at approximately elevation 0.0.

Specifications relating to the berm called for minimum blow counts as recorded from solid stem DPTs, which are used locally as an expedient substitute for SPTs. The required minimum DPT blow counts that are presented in Fig. 5 as functions of depth for several fines contents resulted from the consideration of a seismic shaking of magnitude 7 and acceleration level of 0.3g (NBC 1990; 1 in 475 years event). Because the deep loose sand was shown to generally contain between 5 and 10% fines, the curve shown for the lower fines contents would apply to that layer. The grain size distribution curve available for the deeper sand indicated a D_{50} of approximately 0.3 mm and a clay content less than 8%.

3.2 Field Trials

As for most soil improvement assignments, Franki conducted field trials to establish in situ the procedure (vibrator power, insertion and withdrawal procedure, vibration duration, and probe spacing) able to economically produce the required results. In particular, a test area was selected around Sta 3+50 because of an initially available nearby DPT and boring. Three triangular patterns were completed with a limited number of probing locations at spacings of 3, 2.5 and 1.8 m.

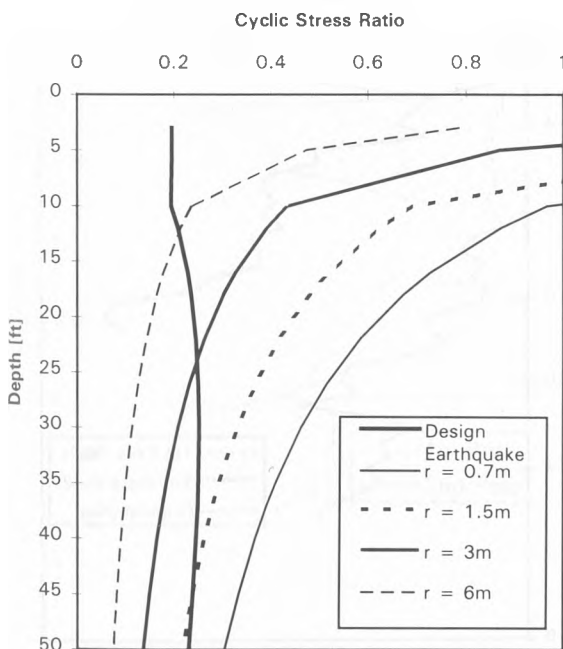


Figure 4. Cyclic Stress Ratio

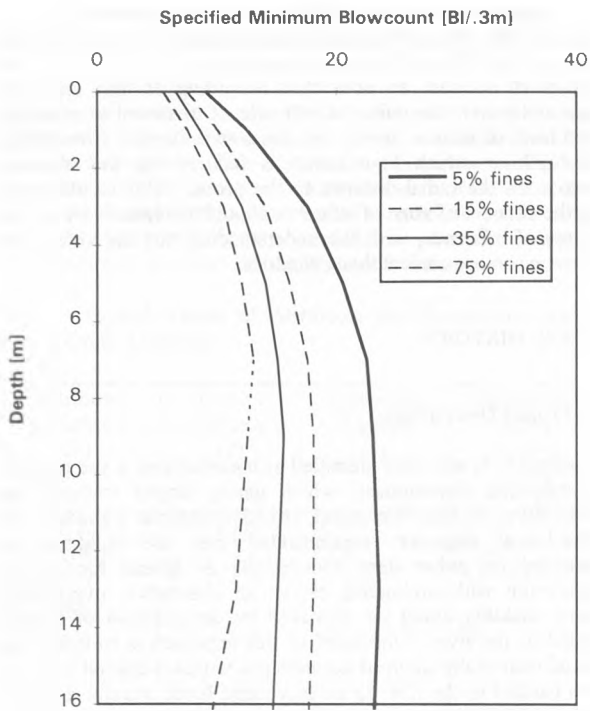


Figure 5. Densification Criteria

The DPT profiles corresponding to the original and treated conditions are shown in Fig. 6, with the nearby available DPT labeled as "initial original". Although it was believed that the control DPTs were performed too soon after probing to allow for the full development of the improvement, the nature of the soil layer is evidenced by the amount of improvement: marginal in the

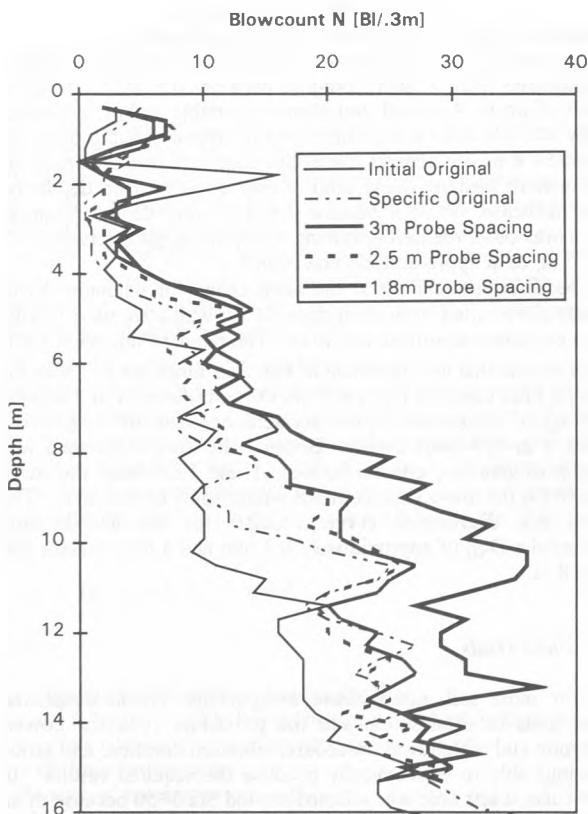


Figure 6. Field Trials DPT Results

75%-fines silt from a depth of 4.4 to 7.0 m and significant in the 5- to 10%-fines sand below that depth.

The "specific original" test, also shown in Fig. 6, was obtained at the specific location of the test area after the trials were completed. Bearing in mind some of the trends highlighted in Fig. 4, it is of interest to note that the larger probe spacings (2.5 and 3 m) produced a noticeable improvement to a depth of approximately 10 m, while the closer spacing of 1.8 m not only increased the improvement ratio within the 10 m depth range, but also resulted in improvement to the maximum depth of 14 m reached by the probe.

3.3 Production Densification

Because the "initial original" test performed as part of the original site investigation was initially used for comparison purposes in the test area mentioned above, an optimistic comparison led to the preliminary conclusion that a 2.5 m spacing would be sufficient to produce the required results. Production densification was therefore started with a near-triangular pattern characterized by a lateral spacing of 2.5 m (base of triangle) between rows and a longitudinal spacing of 2.15 m (height of triangle) between lines. The number of probing locations at each line alternated between 4 and 5, to provide, on average, the lateral coverage specified for the berms.

Control DPTs performed at the center of the triangular pattern cells indicated that the required blow counts were not met, and that a second pass would be needed. Fig. 7 shows the DPT blow counts obtained in the vicinity of Sta 8+12 before (Nb) and after (Na1) the 1st pass (2.5 m spacing). Although the numbers have markedly improved, they do not exceed the required blows counts above 8 m depth shown for the 5%-fines case. Based on these and similar observations conducted at other stations, it was decided to apply a second pass with a depth of approximately 8.5 m (i.e. El -7.00) to the areas to be densified. The application of the second pass resulted in a rectangular pattern with a unit cell of 1.25 x 2.15 m, leading to 9 full rows of probing locations. The additional pass resulted in a doubling of the density of energy delivered to the soil between 0 and 8 m depth.

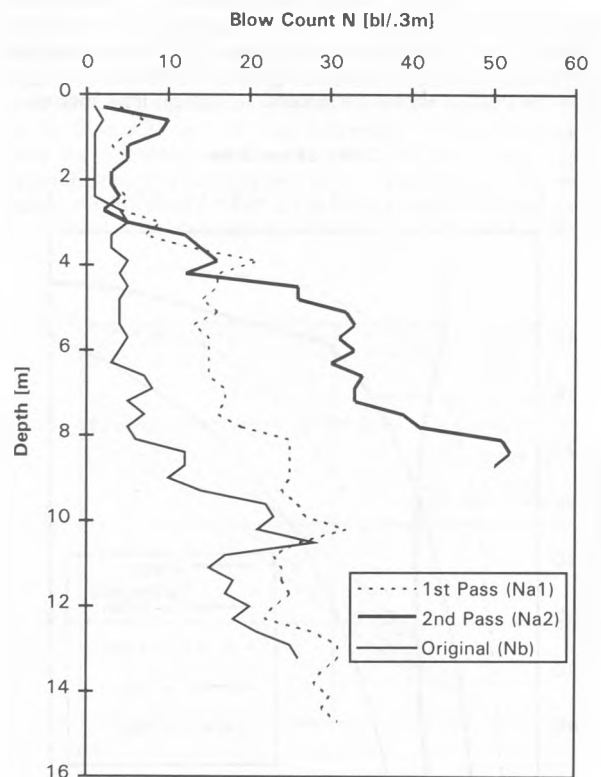


Figure 7. DPT Results @ Station 8+12

Fig. 7 also shows the results (Na2) of a DPT test performed at the center of the rectangular probing cell, i.e. after completion of the second pass, to a depth of 8.6 m (i.e. El -7.00) in the vicinity of Sta 8+12. It can be seen that the level of improvement has substantially increased, to the point that the blow counts specified for the sand layer were exceeded by at least 50%. To develop a more global representation of the relative improvement produced by the Y-probe over the site, several DPT profiles were averaged and compared as functions of depths. Fig. 8 shows the improvement factor obtained by averaging and calculating the ratios of DPTs collected between Sta 6+50 to 9+00; 8 DPTs were used to summarize the original conditions (Nb), 6 DPTs after the 1st pass (Na1), and 4 DPTs after the 2nd pass (Na2).

It can be seen that the improvement factor Na1/Nb is approximately 2 between 4- and 8-m depth and decreases asymptotically at larger depths to reach about 1 at approximately 13 m. This decrease with depth is not attributable to a change in the sand gradation, which is reported to uniformly contain approximately 5 to 8% fines below 7 m. It is believed that this tapering off in improvement factor is probably related to the increase in effective overburden with depth that adversely decreases the potential for liquefaction during vibration - a prerequisite for densification. As shown in Fig. 4, as the horizontal stress increases with depth, the cyclic stress ratio decreases to the point that, below a given depth, the radius of the liquefied zone of influence may become smaller than half the spacing between probing locations.

The improvement factor Na2/Nb exceeds 4 between 5- and 9-m depths, and decreases sharply towards 1 between 9- and 10-m depth. This abrupt decrease is directly related to the depth of the probe insertion during the second pass. The ratio Na2/Na1 is similar to the ratio Na1/Nb in the 3- to 9-m depth range, which seems to indicate that, in this case, improvement factors can be multiplied to reflect superposition of passes.

The lower improvement factors observed at depths shallower than 4 m reflects the influence of the fines content which varies with the nature of the interbedded layers. It is a surprise to note, however, improvement to some degree in the fine grained layer located between 3 and 4 m depth. According to the laboratory analysis performed on several samples collected, this layer is characterized by an average fines content of 45%, a level beyond which liquefaction would not be expected to occur. Even in the

layers containing 80% fines encountered at 1.5 and 2.8 m depth, about a 50% improvement was achieved after the second pass.

These observations would indicate that finer grained soils can liquefy and exhibit improvement if subjected to a very large number of high-strain cycles. The observations also confirm that Y-probe vibrations can induce liquefaction in soil zones that would not normally be considered as liquefiable under the design earthquake.

3.4 CPT and PMT Testing

CPT and PMT testing were performed after completion of the improvement contract in the vicinity of Sta 3+92, at Franki's initiative, to provide correlation between the extensive DPT testing performed as part of the quality control of the site and a more widely used type of test. Although it would have been preferable to establish the correlation in the east berm zone covering the DPTs discussed above, preloading fill had already been placed in the area and it was felt that the effects of the preloading would complicate interpretation of the data.

Correlations are presented in Figs. 9 and 10 corresponding to original (just outside the eastern end of the west berm) and improved soil conditions, respectively. The DPT blow count is plotted as a function of depth along with 2.5 times the CPT cone resistance (q_c) expressed in MPa, and the CPT friction ratio (FR, expressed in thousandths, $[10^{-3}]$). The multiplier factor was chosen in keeping with the generally accepted q_c [tsf] = 4 N_{SPT} , correlating CPT and SPT results in clean medium sands.

Fig. 9 indicates that 2.5 q_c [MPa] correlates reasonably well with the DPT blow counts in the deep sand layer, except for the tendency of the DPT diagram to increase with depth more than the cone resistance diagram. This is understandable in as much as the DPT blow count is representative of the resistance acting on its tip, in addition to the friction accrued along the lateral surface of the rods. Fig. 10 indicates a less convincing correlation and a more pronounced trend of the DPT diagram to increase with depth. Confirmation of the decrease of the improvement with depth discussed above can be noted in Fig. 10.

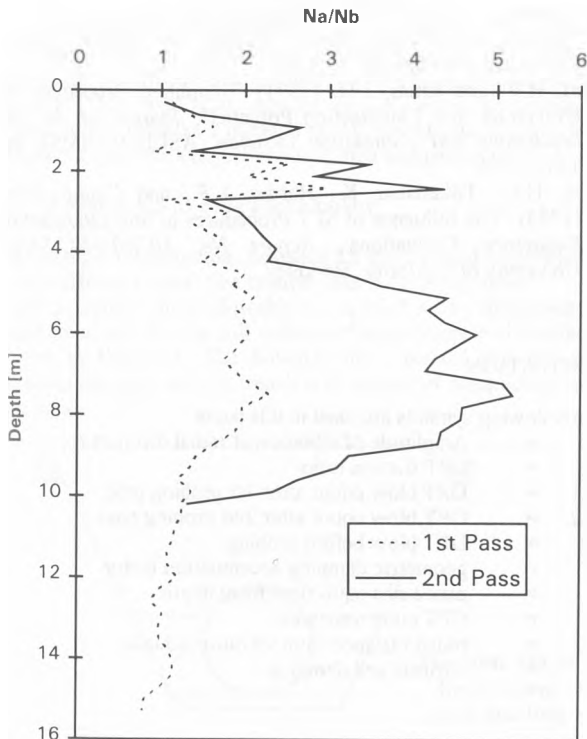


Figure 8. Average Multiplier

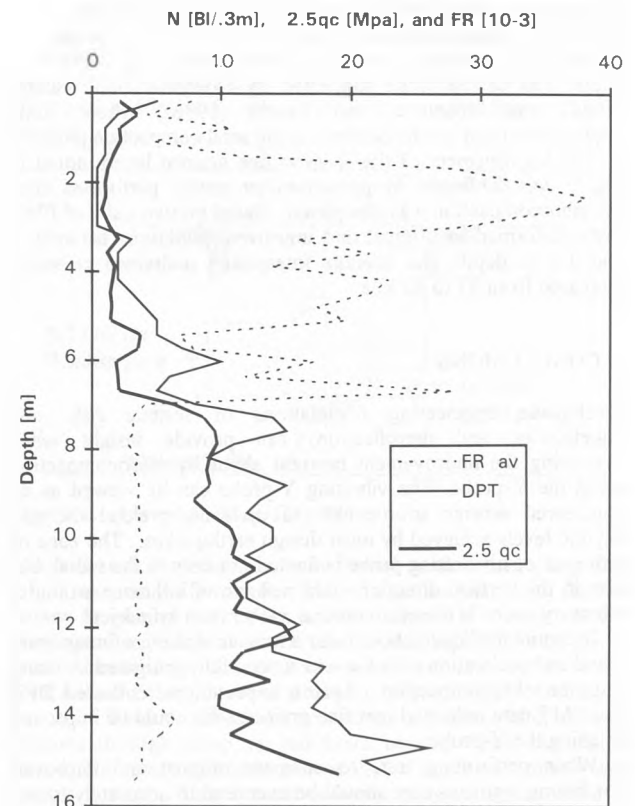


Figure 9. CPT - DPT Correlation for Original Condition

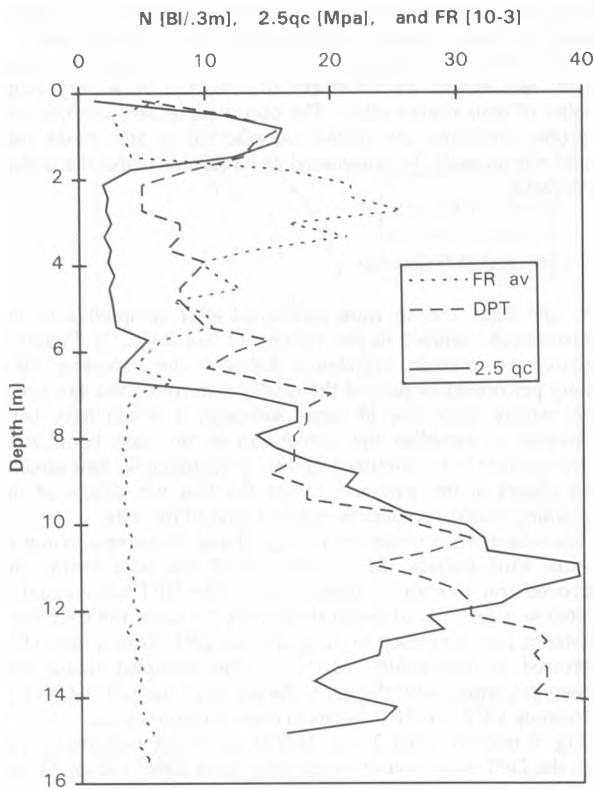


Figure 10. CPT - DPT Correlation for Densified Condition

When comparing Fig. 10 to Fig. 9, it can be seen that, on the average, CPTs better identify localized looser zones while yielding higher local and global improvement factors. It can therefore be concluded that average improvement factors, such as those shown in Fig. 8, are safe estimates when applied to CPT verifications. Cone resistances in the finer grained soils between 2 and 6 m depth increased by approximately 50 %, in spite of friction ratios between 1 and 2%. These friction ratios are at the higher end of the range suggested by Holeyman and Wallays (1984) and Holeyman and Broms (1986), where some improvement can still be obtained using sand compaction piles.

The improvement of the shallow fine grained layers noted in Fig. 7 was confirmed by pressuremeter testing performed after the vibrocompaction was completed. Based on two pairs of PMT tests performed in original and improved conditions between 2 and 3.2 m depth, the average interpreted undrained cohesion increased from 37 to 43 kPa.

4 CONCLUSIONS

Earthquake engineering (evaluations of seismic risk, soil liquefaction, and densification) can provide insight when evaluating the improvement brought about by vibrocompaction using the Y-probe. The vibrating Y-probe can be viewed as an engineered seismic source able to cyclically preload the soil beyond levels achieved by most design earthquakes. The zone of influence of a vibrating probe is limited not only in the radial, but also in the vertical direction. The volume of influence around a vibratory probe is therefore conical, rather than cylindrical.

Potential for liquefaction under a seismic shaking of magnitude 7 and an acceleration of 0.3 g was successfully mitigated by using Y-probe vibrocompaction. Against expectations, collected DPT and PMT data indicated that fine grained soils could be improved by using the Y-probe.

When performing tests to compare original and improved conditions, rigorous care should be exercised to accurately locate soundings with respect to the probing pattern, and to enforce - sometimes against the client's burning impatience - a proper rest period between treatment and testing. When compared to DPT

data, CPT data tend to provide a more detailed local, yet more optimistic average characterization of soil densification. The Y-probe has potential as a research tool for the in situ study of soil liquefaction.

5 ACKNOWLEDGMENTS

The Y-probe field trials results, production data, and site properties referred to in this paper were provided by Franki Canada, through Mr. John Kennedy. The writer wishes to thank Dr. William Neely, VSL Corporation, and Mrs. Elsie Kent for their valuable review comments.

6 REFERENCES

- Campbell, K. W. (1981) "Near-Source Attenuation of Peak Horizontal Acceleration", *Bulletin of the Seismological Society of America*, vol 71, pp. 2039-2070.
- Finn, W.D., Martin, G.R., and Lee, K.L. (1978) "Comparison of Dynamic Analyses for Saturated Sands", *Proceedings of the ASCE Specialty Conference on Earthquake Engineering and Soil Dynamics*, Vol. 1, pp. 472-491, ASCE, New York.
- Holeyman, A. and Wallays, M. (1984) "Compaction par damage en profondeur", *Proceedings of the International Conference on In Situ Soil and Rock Reinforcement*, Paris, October 1984, pp. 367-372, (in French).
- Holeyman, A. and Broms, B. (1986) "Sand Compaction Piles", *Proceedings of the International Conference on Deep Foundations*, Peking, September 1986, Vol. II, pp. 2.26-2.31.
- Mitchell, J.K. (1982) "Soil Improvement - State-of-the-art Report", *Proceedings of the Tenth International Conference on Soil Mechanics and Foundation Engineering*, Vol. 4, pp. 509-565, June 1981, Stockholm, Balkema.
- Mualchin, L. and Jones, A., L. (1992) "Peak Acceleration from Maximum Credible Earthquakes in California (Rock and Stiff-oil Sites)", *DMG Open-File Report 92-1*, Division of Mines and Geology, Sacramento, California.
- Neely, W.J. and Leroy, D.A. (1991) "Densification of Sand using a Variable Frequency Vibratory Probe", *ASTM Special Technical Publication 1089*, pp. 320-332.
- Schnabel, P. B., Lysmer, J., and Seed, H.B. (1972) "SHAKE: A computer Program for Earthquake Response Analysis of Horizontally Layered Sites", *Report No. EERC 72-12*, University of California, Berkeley.
- Seed, H.B. and Idriss, I.M. (1971) "Simplified Procedure for Evaluating Soil Liquefaction Potential", *Journal of the Soil Mechanics and Foundation Division*, ASCE 97(SM9), pp. 1249-1273.
- Seed, H.B., Tokimatsu, K., Harder, L.F., and Chung, R.M. (1984) "The Influence of SPT Procedures in Soil Liquefaction Resistance Evaluations", *Report No. UCB/EERC-84/15*, University of California, Berkeley.

7 NOTATION

The following symbols are used in this paper:

- A_r = Amplitude of vibration at radial distance r
 FR = CPT friction ratio
 $Na1$ = DPT blow count after 1st probing pass
 $Na2$ = DPT blow count after 2nd probing pass
 N_b = DPT blow before probing
 b = geometric damping accentuation factor
 h = probe ribs equivalent focal depth
 qc = CPT cone resistance
 r = radial distance from vibration source
 a = intrinsic soil damping